Northern Galápagos corals reveal twentieth century warming in the eastern tropical Pacific

Northern Galápagos corals reveal twentieth century warming in the eastern tropical Pacific

Gloria Jimenez[1]*, Julia E. Cole[2], Diane M. Thompson[3], Alexander W. Tudhope[4]

[1]Department of Geosciences, University of Arizona, Tucson, Arizona, USA. [2]Department of Earth and Environmental Sciences, University of Michigan, Ann Arbor, USA [3]Department of Earth and Environment, Boston University, Boston, Massachusetts, USA. [4]School of GeoSciences, University of Edinburgh, Edinburgh, UK.

Corresponding author: Gloria Jimenez (jimenezgloria@email.arizona.edu)

Key Points:

- A new coral Sr/Ca record from Wolf Island, Galápagos indicates SST warming on decadal to multidecadal timescales.
- Trend analysis of multiple datasets confirms long-term warming throughout the eastern tropical Pacific, consistent with radiative forcing.
- Eastern Pacific warming since 1982 is overprinted by seasonally variable cooling from wind forcing and the ocean dynamical thermostat.

This article has been accepted for publication and undergone full peer review but has not been through the copyediting, typesetting, pagination and proofreading process which may lead to differences between this version and the Version of Record. Please cite this article as doi: 10.1002/2017GL075323

Abstract

Models and observations disagree regarding sea surface temperature (SST) trends in the eastern tropical Pacific (ETP). We present a new Sr/Ca-SST record that spans 1940-2010 from two Wolf Island corals (northern Galápagos). Trend analysis of the Wolf record shows significant warming on multiple timescales, which is also present in several other records and gridded instrumental products. Together, these datasets suggest that most of the ETP has warmed over the 20th century. In contrast, recent decades have been characterized by warming during boreal spring and summer (especially north of the equator), and subtropical cooling during boreal fall and winter (especially south of the equator). These SST trends are consistent with the effects of radiative forcing, mitigated by cooling due to wind forcing during boreal winter, as well as intensified upwelling and a strengthened Equatorial Undercurrent.

1 Introduction

Broad evidence suggests that the mean state of the tropical Pacific Ocean has changed throughout the 20th century in response to rising greenhouse gas concentrations (Karnauskas et al., 2009; Yeh et al., 2009; Collins et al., 2010; DiNezio et al., 2010; Capotondi et al., 2015). Warming is clear over most of the basin, but attempts to relate warming to particular mechanisms have yielded competing conceptual models. The “weaker Walker” model holds that atmospheric warming produces greater increases in water vapor relative to precipitation, causing reduced vertical vapor transport (Held and Soden, 2006). Via the Bjerknes feedback, this would slow the easterly trade winds, weakening oceanic circulation and upwelling and leading to warming across the tropical Pacific (Vecchi and Soden, 2007; Collins et al., 2010; Cai et al., 2015). Alternatively, the ocean dynamical thermostat (ODT) model suggests that the eastern and western Pacific should experience differential warming: increased upwelling in the east should strengthen the zonal sea surface temperature (SST) gradient and the Walker circulation, amplifying the trades and damping warming in the eastern and central Pacific (Clement et al., 1996). A third model posits that evaporative heat loss should be more efficient in areas of low humidity or strong winds, thus predicting greater equatorial warming relative to the subtropics and in the western relative to the eastern Pacific (Vecchi et al., 2008; DiNezio et al., 2009; Xie et al., 2010).

Evaluating these hypotheses is difficult because observations remain ambiguous regarding the nature and direction of SST trends in the eastern tropical Pacific (ETP) (DiNezio et al., 2009; Sayani et al., 2011; An and Im, 2013; Abram et al., 2016). In-situ (e.g., Wolff, 2010), instrumental (Deser et al., 2010b), and proxy records (Tierney et al., 2015) do not agree on the climatic history of the region, and models reproduce SST patterns poorly (Vecchi et al., 2008).

Paleoclimate data can help overcome the region’s paucity of instrumental climate records. Previous work has leveraged data from the Galápagos archipelago, where geochemical records from corals extend the observational baseline provided by in-situ data beginning in the mid-1960s (Wolff, 2010). However, highly variable SST associated with El Nino challenges coral survival. In particular, the extreme 1982-83 El Niño event caused coral reef mortality of up to 97% (Glynn et al., 2015). Thus, despite a long history of coral paleoclimatology in the Galápagos, existing records stop in 1982 (e.g., Shen et al., 1992;

Dunbar et al., 1994; Guilderson and Schrag, 1998) and do not show modern trends (Cole and Tudhope, 2016).

As a result, SST trends in the Galápagos are still debated. While some studies suggest neutral or cooling SSTs during the late 20th century (Wolff, 2010; Karnauskas et al., 2015b), others show a stepwise SST increase following the 1976 Pacific climate shift (Guilderson and Schrag, 1998) or even suggest that warming began before the 20th century (Conroy et al., 2009).

Here, we present a new SST reconstruction that spans 1940-2010 from two Wolf Island corals, in the northern Galápagos archipelago (Fig. 1). Our record is the first from Galápagos to bridge the 1982-83 event. Together with other coral, instrumental, and satellite-based gridded datasets, we use this record to investigate 20th century SST trends throughout the ETP. The spatial patterns of recent trends allow us to assess the mechanisms controlling the trajectory of the tropical Pacific's response to climate change.

2 Data and Methods

2.1 ETP climatology and oceanographic setting

The Galápagos archipelago lies 1000 km west of South America (Fig. 1). The large southern islands sit atop the Galápagos platform (Fig. 1b), which impedes the eastward-flowing Equatorial Undercurrent (EUC), inducing upwelling of cold, saline water, particularly from July-September (Kessler, 2006). Wolf (Wenman) Island is approximately 150 km north of the main Galápagos platform; it experiences less topographic upwelling and has a climatology more characteristic of the surrounding ocean (see supporting information; Sweet et al., 2007). Wolf Island corals have recovered from the 1982-83 and 1997-98 El Niños to a greater extent than those in the southern islands (Glynn et al., 2015).

The pattern of ETP SSTs (Fig. 1a; Supporting Information S1) reflects a seasonal interplay between atmospheric and oceanic dynamics, integrating the cooling effects of upwelling and warming from off-equatorial and atmospheric sources (Toggweiler and Dixon, 1991; Zhang and McPhaden, 1995; Fiedler and Talley, 2006; Kessler, 2006). From June-December, increased winds drive cooling via equatorial upwelling; combined with strengthening of the South Equatorial Current and North Equatorial Countercurrent, this causes warming north of the equatorial front and cooling to the south (Fig. S1; Julian and Chervin, 1978; Lukas, 1986; Wallace et al., 1989; Strub et al., 1998; Johnson et al., 2002; Kessler, 2006). SST cooling from equatorial upwelling is controlled by the seasonal cycle of the thermocline, which makes cold water available for wind mixing when it shoals between June and September (from 50 to 30 m near 95°W) (Kessler, 2006).

2.2 Coral collection and sampling

In May-June 2010, we cored two living Porites lobata corals from Shark Bay (Glynn et al., 2015), along the northeastern shore of Wolf Island, Galápagos (1º23.15' N, 91º49.90' W). The cores span 71 and 35 years (see Fig. 2). Cores were slabbed, X-rayed, and subsampled with a computer-controlled micromill at 1 mm resolution. We measured Sr/Ca ratios using

ICP-AES (Schrag, 1999). Supporting Information S1 gives a detailed description of sampling methods, including skeletal examination (DeLong et al., 2007; Sayani et al., 2011; DeLong et al., 2012), age modeling (Howell et al., 2006), creation of a composite record (Mann and Jones, 2003), and Sr/Ca-SST calibration and uncertainty calculations (Corrège, 2006; Linsley et al., 2008; Nurhati et al., 2011; Thirumalai et al., 2011; Gagan et al., 2012).

2.3 Trend analysis

We analyzed SST trends in tropical year-averaged (April-March) versions of the Wolf reconstruction and several other series. We used the SIgnificant ZERo crossings of derivatives (SiZer) method (Chaudhuri and Marron, 1999; Hannig and Marron, 2006; Abram et al., 2016), which separates important structural features of a time series from noise by applying multiple Gaussian kernel filters to a time series to yield a family of smoothed series. SiZer then identifies regions with statistically significant slopes in these series; critically, the calculation of significance for a given point accounts for its location and the resolution at which the series is examined (Chaudhuri and Marron, 1999). This approach helps avoid trend sensitivity to endpoints (e.g., Karnauskas et al., 2015a).

Following Abram et al. (2016), we applied filter widths from 5-50 years and assessed significance for $p<0.1$. We evaluated the presence of a long-term and a decadal trend (50- and 10-year filter widths, respectively), which we termed sustained if they persisted to the end of the series (Abram et al., 2016).

We applied the same methodology to several other 20th century ETP SST datasets (Fig. 1). These include coral Sr/Ca-SST records from Clipperton Atoll (Wu et al., 2014) and Palmyra Island (Nurhati et al., 2011) and instrumental data from Puerto Ayora (Wolff, 2010) and Puerto Chicama (K. Takahashi, pers. comm.).

To place these records in spatial context, we mapped linear trends in gridded datasets. For recent trends (1982-2014), we used the 0.25° Optimum Interpolation Sea Surface Temperature (OISST) dataset (Reynolds et al., 2007); this spatial resolution emphasizes small-scale differences. While these high-resolution data are not available prior to the satellite era, coarser products can still provide insight on long-term trends. We evaluated the trend from 1900-2014 using the 2° Extended Reconstructed Sea Surface Temperature v4 (ERSST4) dataset, which generally reproduces early-20th century El Niño-Southern Oscillation (ENSO) variability despite sparse data (Huang et al., 2015), and minimizes the cooling bias present in many gridded datasets since 2003 (Hausfather et al., 2017).

3 Results

3.1 Wolf Island composite SST reconstruction

The SST reconstruction from Wolf Island spans 1940-2010 with an average resolution of 16 samples per year (Fig. 2 and Tables S1-S2). Both corals that contributed to the composite record have a growth hiatus from 1983 to 1985; they correlate well over their period of overlap ($r=0.71$). We present the record interpolated to bimonthly resolution; the tropical year-averaged record correlates significantly ($p<0.001$) with gridded instrumental SST products centered over Wolf Island (OISST: $r=0.82$ and ERSST4: $r=0.57$). The pattern of correlation between the Wolf composite and SST highlights its sensitivity to ENSO (Fig. S4).

3.2 SST trends in ETP records

We found significant warming trends in all the coral-based SST records. From 1940-2010, the Wolf SST reconstruction has a linear trend of 1.19°C ± 0.31°C (0.17°C/decade). SiZer analysis identifies a significant long-term warming trend (50-year filter width) throughout the Wolf and Clipperton records, and after 1900 at Palmyra (Figs. 3, S5; see Supporting Information S1 and Fig. S6 for an analysis of the individual Wolf cores). Significant and sustained decadal warming (10-year filter width) is focused in the latter part of all three records, beginning in 1979, 1972, and 1988, respectively. However, we find no significant trends in the Puerto Ayora and Puerto Chicama instrumental records (Fig. 3). At Wolf, the warming trend begins shortly after a widespread shift to decadally warmer conditions in 1976 (consistent with Guilderson and Schrag (1998)), though the short length of the record precludes an in-depth analysis of the Pacific decadal signal.

3.3 Spatial patterns in ETP SST trends

There is a significant linear warming trend in ERSST4 over most of the ETP from 1900-2014, ranging from 0.05-0.1°C/decade (Fig. 4a). In contrast, more recent (1982-2014) ETP OISST trends are spatially heterogeneous (Fig. 4b). Warming (up to 0.3°C per decade) is concentrated off-equator, including the eastern Pacific warm pool near Clipperton. Cooling is present in the subtropics, forming a wedge pointing west. Along the equator, annual SST trends show a hemispheric division with a warming tendency north of the equator (approximately 0.1°C/decade) and cooling south of the equator and near the Galápagos cold pool (0.2-0.1°C/decade). These SST trends vary seasonally: cooling is prominent during DJF, but there is a warming tendency during the remaining seasons, particularly north of the equator (Fig. 5).

4 Discussion

4.1 Reliability of the Wolf record

Several quality controls on the Wolf SST reconstruction suggest that the data faithfully reflect SST. SEM images show no alteration in the areas of the coral skeletons sampled for Sr/Ca (Fig. S2). Additionally, the two cores comprising the reconstruction agree closely with each other and with gridded data (Supporting Information S1), in contrast to other sites where replication is a concern (Alpert et al., 2016) or vital effects may exert a strong control on coral Sr/Ca (DeCarlo et al., 2015; 2016). Finally, calibration parameters for both cores resemble previously published equations (Table S1).

4.2 Trend stability

We consider the SiZer trend results highly robust; the results (Fig. 3) do not change if different endpoints are chosen. An exception is at Palmyra, where high decadal variability means that trimming the series can affect the significance of the long-term trend.

Because decadal variability can influence linear trend calculations (e.g., L'Heureux et al., 2012), we selected multidecadal intervals to minimize trend sensitivity. For the recent decadal trends, time intervals <20 years yielded unstable results. Therefore, we calculated trends over the longest time interval that included high-resolution satellite data and did not end during the 2015-2016 El Niño (1982-2014). Over both time intervals we analyzed, the resulting trends are insensitive to endpoint variations (for example, trend maps are similar with any endpoints from 1982-1984 and 2011-2014).

4.3 Coherent patterns in ETP SST trends

On multidecadal timescales, both SiZer and linear trends suggest that much of the ETP has warmed over the 20th century. ERSST4 shows a basin-wide warming trend and SiZer analysis indicates significant long-term warming in the Wolf, Clipperton, and Palmyra records.

This conclusion is supported by other studies. Deser et al. (2010a) showed 20th century ETP warming in most datasets they examined (including those with no interpolation), and L'Heureux et al. (2012) found a positive trend in the canonical El Niño pattern of SST variability from 1950-2010. Using paleoclimate data, Tierney et al. (2015) found that eastern Pacific warming began in 1913; climate model simulations by Abram et al. (2016) showed warming beginning in the early 20th century. Exceptions occur at Puerto Ayora and Puerto Chicama, where SiZer analysis finds no significant trends but linear trends in ERSST4 indicate warming (Figs. 3, 4a). The SiZer results are consistent with previous observational and modeling work (Wolff, 2010; Gutiérrez et al., 2011; Dewitte et al., 2012). Similarly, models and gridded data (including earlier versions of ERSST4) often fail to reproduce observed cooling along the Peruvian coast (Falvey and Garreaud, 2009). We conclude that these areas are probably experiencing a neutral to cooling trend on multidecadal timescales.

Recent decadal trends (1982-2014) are spatially heterogeneous (Fig. 4b), but largely coincide with SiZer results (Fig. 3) and with previous work. Our recent trend maps (Figs. 4b and 5) support previous interpretations that the Interdecadal Pacific Oscillation plays an important role in the region's recent SST trends (England et al., 2014; Thompson et al., 2015).

We also observe a cooling tendency around the Galápagos cold pool (Figs. 4b and 5), in agreement with Karnauskas et al. (2015b), who showed that the cold pool has intensified and expanded northward since 1982. However, the Wolf record, together with Fig. 4b, suggests that this cooling trend does not reach the northern Galápagos islands (Wolf and Darwin). Finally, the seasonal trends in Fig. 5 generally match the conclusions of Amaya et al. (2015), who found equatorial Pacific SST cooling during DJFMAM and warming during JJASON from 1990-2009.

4.4 Mechanisms driving ETP SST trends

This trend analysis allows us to evaluate the mechanisms governing recent ETP SSTs. Over the 20th century, the uniform multidecadal warming trend in Fig. 4a, along with SiZer analysis of the Wolf, Clipperton, and Palmyra coral records, suggests that radiative forcing has resulted in pervasive warming throughout the ETP except for immediately adjacent to the

South American coast. We observe no clear relationship between trends in winds and SST over the 20th century (Fig. 4a).

In contrast, the complex SST trends from 1982-2014 suggest the involvement of ocean-atmosphere dynamics (Figs. 4b, 5). The trend pattern is broadly consistent with the ODT hypothesis (Clement et al., 1996), which predicts that strong upwelling during SON should oppose radiative forcing, leading to equatorial SST cooling, while the ODT should lose efficiency during spring, leading to warming. These predictions largely match Fig. 5, which shows equatorial Pacific cooling during SON and especially DJF, and warming beginning in MAM and strengthening in JJA.

Wind forcing is a component of the ODT hypothesis that has been implicated as a driver of recent ETP SST trends in both observational (England et al., 2014) and modeling (Xie et al., 2010) studies, especially in the southeastern subtropics. While Fig. 5 shows that cooling coincides with strengthened winds during DJF, the link between winds and SST is otherwise weak, suggesting seasonally variable interactions between wind forcing and the ODT. The difference in annual wind trends between Figs. 4a and 4b suggests that the more recent trends integrate variability from decadal-scale forcings.

Additionally, a strengthened EUC would enhance ODT effects south of the equator. Drenkard and Karnauskas (2014) showed a significant increase in EUC velocity since the 19th century using ocean reanalysis data, and Amaya et al. (2015) found that the EUC's core had intensified from 1990-2009. The resulting upwelling explains cooling along and south of the equatorial front in maps of annual and SON trends (Figs. 4b, 5c) and in the Galápagos cold pool (Karnauskas et al., 2015b).

5 Conclusions

Our new coral-based SST record from Wolf Island (1940-2010) shows significant SST warming on decadal to multidecadal timescales. Along with other coral and instrumental records and gridded datasets, the Wolf record confirms widespread 20th century ETP warming, with exceptions near the Galápagos cold pool and along the South American coast. Recent decades (1982-2014) display large spatial and temporal variability in ETP SST trends, with warming during boreal spring and summer, and cooling during fall and winter (particularly south of the equator).

We conclude that on multidecadal timescales, the ETP has warmed in response to radiative forcing. On shorter timescales, recent SST trends integrate seasonally fluctuating oceanic and atmospheric drivers. During SON and DJF, stronger wind-driven upwelling (as predicted by the ODT hypothesis) produces cooling. EUC strengthening further cools SSTs south of the equator, resulting in a hemispheric trend pattern, and this cooling is also amplified by increased winds during DJF. In contrast, during MAM and JJA, weaker upwelling and winds allow other factors to predominate, such as zonal advection of warm water (Amaya et al., 2015).

This spatial heterogeneity in recent ETP SST trends implies that large-scale analyses may mask important regional and seasonal distinctions. Our results suggest that analyses of zonal and meridional gradients should explicitly consider regional and seasonal forcings to avoid excluding or emphasizing particular (internal or external) forcing mechanisms.

Finally, warming at Wolf Island has important implications for management of the Parque Nacional Galápagos, a World Heritage site and a critical source of tourism revenue for Ecuador. Previous work has proposed that increased topographic upwelling due to EUC strengthening may shield Galápagos and other Pacific islands from the full extent of radiative warming (Karnauskas and Cohen, 2012; Karnauskas et al., 2016). Although regions in the southern Galápagos may be insulated from warming due to nearby upwelling centers (Karnauskas et al., 2015b), our results suggest that this protection does not extend throughout the archipelago. The northern islands, which are experiencing warming, host some of the only long-lived healthy corals in the park. These corals may be more vulnerable to global warming than previously thought.

Acknowledgments, Samples, and Data

Detailed descriptions of all laboratory and data analyses can be found in Supporting Information S1. We thank the Charles Darwin Station and the Parque Nacional Galápagos, particularly Galo Quezada, for permitting and facilitating coral collection, and Colin Chilcott, Roberto Pepolas, Diego Ruiz, Jenifer Suarez, and the captain and crew of the Queen Mabel for help with fieldwork. We are also grateful to Ken Takahashi for providing data from Puerto Chicama; Stephan Hlohowskyj, Sydnie Lemieux, and Keeley Lyons-Letts for laboratory assistance; Kevin Anchukaitis and Luke Parsons for analytical advice; and Lael Vetter for thoughtful discussion. This work is supported by National Science Foundation grants #1401326 and #0957881 to JEC; UK Natural Environment Research Council grant NE/H009957/1 to AT; and a National Science Foundation Graduate Research Fellowship and Philanthropic Education Organization Fellowship to GJ. The data associated with this manuscript is available at the NOAA National Centers for Environmental Information Paleoclimatology website. We declare no competing financial interests.

References

Abram, N. J., H. V. McGregor, J. E. Tierney, M. N. Evans, N. P. McKay, D. S. Kaufman, and K. Thirumalai (2016), Early onset of industrial-era warming across the oceans and continents, Nature, 536(7617), 411–418, doi:10.1038/nature19082.

Alpert, A. E., A. L. Cohen, D. W. Oppo, T. M. DeCarlo, J. M. Gove, and C. W. Young (2016), Comparison of equatorial Pacific sea surface temperature variability and trends with Sr/Ca records from multiple corals, Paleoceanography, 31(2), 252–265, doi:10.1002/2015PA002897.

Amaya, D. J., S.-P. Xie, A. J. Miller, and M. J. McPhaden (2015), Seasonality of tropical Pacific decadal trends associated with the 21st century global warming hiatus, J. Geophys. Res. Oceans, 120(10), 6782–6798, doi:10.1002/2015JC010906.

An, S.-I., and S.-H. Im (2013), Blunt ocean dynamical thermostat in response of tropical eastern Pacific SST to global warming, Theor Appl Climatol, 118(1-2), 173–183, doi:10.1007/s00704-013-1048-0.

Cai, W. et al. (2015), ENSO and greenhouse warming, Nature Climate change, 5(9), 849–859, doi:10.1038/nclimate2743.

Capotondi, A. et al. (2015), Understanding ENSO Diversity, Bull. Amer. Meteor. Soc., 96(6), 921–938, doi:10.1175/BAMS-D-13-00117.1.

Chaudhuri, P., and J. S. Marron (1999), SiZer for Exploration of Structures in Curves, Journal of the American Statistical Association, 94(447), 807–823, doi:10.1080/01621459.1999.10474186.

Clement, A. C., R. Seager, and M. A. Cane (1996), An ocean dynamical thermostat, Journal of Climate, 9, 2190–2196, doi:10.1175/1520-0442(1996)009<2190:AODT>2.0.CO;2.

Cole, J. E., and A. W. Tudhope (2016), Reef-based reconstructions of eastern Pacific climate variability, in Coral Reefs of the Eastern Tropical Pacific: Persistence and Loss in a Dynamic Environment, edited by P. W. Glynn and D. Manzello, pp. 535–548.

Collins, M. et al. (2010), The impact of global warming on the tropical Pacific Ocean and El Niño, Nature Geoscience, 3(6), 391–397, doi:10.1038/ngeo868.

Compo, G. P. et al. (2011), The Twentieth Century Reanalysis Project, Quarterly Journal of the Royal Meteorological Society, 137(654), 1–28, doi:10.1002/qj.776.

Conroy, J. L., A. Restrepo, J. T. Overpeck, M. Steinitz-Kannan, J. E. Cole, M. B. Bush, and P. A. Colinvaux (2009), Unprecedented recent warming of surface temperatures in the eastern tropical Pacific Ocean, Nature Geoscience, 2(1), 46–50, doi:10.1038/ngeo390.

Corrège, T. (2006), Sea surface temperature and salinity reconstruction from coral geochemical tracers, Palaeogeography, Palaeoclimatology, Palaeoecology, 232(2-4), 408–428, doi:10.1016/j.palaeo.2005.10.014.

DeCarlo, T. M., G. A. Gaetani, A. L. Cohen, G. L. Foster, A. E. Alpert, and J. A. Stewart (2016), Coral Sr-U thermometry, Paleoceanography, 1–13, doi:10.1002/(ISSN)1944-

9186.

DeCarlo, T. M., G. A. Gaetani, M. Holcomb, and A. L. Cohen (2015), Experimental determination of factors controlling U/Ca of aragonite precipitated from seawater: Implications for interpreting coral skeleton, Geochimica et Cosmochimica Acta, 162(C), 151–165, doi:10.1016/j.gca.2015.04.016.

DeLong, K. L., T. M. Quinn, and F. W. Taylor (2007), Reconstructing twentieth-century sea surface temperature variability in the southwest Pacific: A replication study using multiple coral Sr/Ca records from New Caledonia, Paleoceanography, 22(4), n/a–n/a, doi:10.1029/2007PA001444.

DeLong, K. L., T. M. Quinn, F. W. Taylor, C.-C. Shen, and K. Lin (2012), Improving coral-base paleoclimate reconstructions by replicating 350years of coral Sr/Ca variations, Palaeogeography, Palaeoclimatology, Palaeoecology, 1–19, doi:10.1016/j.palaeo.2012.08.019.

Deser, C., A. S. Phillips, and M. A. Alexander (2010a), Twentieth century tropical sea surface temperature trends revisited, Geophys. Res. Lett., 37(10), doi:10.1029/2010GL043321.

Deser, C., M. A. Alexander, S.-P. Xie, and A. S. Phillips (2010b), Sea Surface Temperature Variability: Patterns and Mechanisms, Annu. Rev. Marine. Sci., 2(1), 115–143, doi:10.1146/annurev-marine-120408-151453.

Dewitte, B. et al. (2012), Change in El Niño flavours over 1958–2008: Implications for the long-term trend of the upwelling off Peru, Deep Sea Research Part II: Topical Studies in Oceanography, 77-80, 143–156, doi:10.1016/j.dsr2.2012.04.011.

DiNezio, P. N., A. C. Clement, and G. A. Vecchi (2009), Climate response of the equatorial Pacific to global warming, J. Climate, 22(18), 4873–4892, doi:10.1175/2009JCLI2982.1.

DiNezio, P., A. Clement, and G. Vecchi (2010), Reconciling Differing Views of Tropical Pacific Climate Change, Eos, Transactions American Geophysical Union, 91(16), 1–3.

Drenkard, E. J., and K. B. Karnauskas (2014), Strengthening of the Pacific Equatorial Undercurrent in the SODA Reanalysis: Mechanisms, Ocean Dynamics, and Implications, J. Climate, 27(6), 2405–2416, doi:10.1175/JCLI-D-13-00359.1.

Dunbar, R. B., G. M. Wellington, M. W. Colgan, and P. W. Glynn (1994), Eastern Pacific sea surface temperature since 1600 A.D.: The δ18O record of climate variability in Galápagos Corals, Paleoceanography, 9(2), 291–315, doi:10.1029/93PA03501.

England, M. H., S. McGregor, P. Spence, and G. A. Meehl (2014), Recent intensification of wind-driven circulation in the Pacific and the ongoing warming hiatus, Nature Climate Change, 4(3), 222–227, doi:10.1038/nclimate2106.

Falvey, M., and R. D. Garreaud (2009), Regional cooling in a warming world: Recent temperature trends in the southeast Pacific and along the west coast of subtropical South America (1979–2006), Journal of Geophysical Research, 114(D4), D04102, doi:10.1029/2008JD010519.

Fiedler, P. C., and L. D. Talley (2006), Hydrography of the eastern tropical Pacific: A review, Progress in Oceanography, 69(2-4), 143–180, doi:10.1016/j.pocean.2006.03.008.

Gagan, M. K., G. B. Dunbar, and A. Suzuki (2012), The effect of skeletal mass accumulation in Porites on coral Sr/Ca and δ18O paleothermometry, Paleoceanography, 27(1), 1–16, doi:10.1029/2011PA002215.

Glynn, P. W., B. Riegl, S. Purkis, J. M. Kerr, and T. B. Smith (2015), Coral reef recovery in the Galápagos Islands: the northernmost islands (Darwin and Wenman), Coral Reefs, 34(2), 1–16, doi:10.1007/s00338-015-1280-4.

Guilderson, T. P., and D. P. Schrag (1998), Abrupt Shift in Subsurface Temperatures in the Tropical Pacific Associated with Changes in El Niño, Science, 281(5374), 240–243, doi:10.1126/science.281.5374.240.

Gutiérrez, D. et al. (2011), Coastal cooling and increased productivity in the main upwelling zone off Peru since the mid-twentieth century, Geophys. Res. Lett., 38(7), 1–6, doi:10.1029/2010GL046324.

Hannig, J., and J. S. Marron (2006), Advanced distribution theory for SiZer, Journal of the American Statistical Association, 101(474), 484–499, doi:10.1198/016214505000001294.

Hausfather, Z., Hausfather, Z., K. Cowtan, K. Cowtan, D. C. Clarke, D. C. Clarke, P. Jacobs, M. Richardson, and R. Rohde (2017), Assessing recent warming using instrumentally homogeneous sea surface temperature records, Science, 3(1), e1601207, doi:10.1126/sciadv.1601207.

Held, I. M., and B. J. Soden (2006), Robust responses of the hydrological cycle to global warming, J. Climate, 19(21), 5686–5699, doi:10.1175/JCLI3990.1.

Howell, P., N. Pisias, J. Ballance, J. Baughman, and L. Ochs (2006), ARAND Time-Series Analysis Software, Available from: http://www.cricyt.edu.ar/paleo/softlib/arand/arand.html (Accessed 19 October 2015)

Huang, B., V. F. Banzon, E. Freeman, J. Lawrimore, W. Liu, T. C. Peterson, T. M. Smith, P. W. Thorne, S. D. Woodruff, and H.-M. Zhang (2015), Extended Reconstructed Sea Surface Temperature Version 4 (ERSST.v4). Part I: Upgrades and Intercomparisons, J. Climate, 28(3), 911–930, doi:10.1175/JCLI-D-14-00006.1.

Johnson, G. C., B. M. Sloyan, W. S. Kessler, and K. E. McTaggart (2002), Direct measurements of upper ocean currents and water properties across the tropical Pacific during the 1990s, Progress in Oceanography, 52(1), 31–61, doi:10.1016/S0079-6611(02)00021-6.

Julian, P. R., and R. M. Chervin (1978), A study of the Southern Oscillation and Walker Circulation phenomenon, Mon. Wea. Rev., 106, 1433–1451, doi:10.1175/1520-0493(1978)106<1433:ASOTSO>2.0.CO;2.

Karnauskas, K. B., A. L. Cohen, and E. J. Drenkard (2015a), Comment on Equatorial Pacific coral geochemical records show recent weakening of the Walker circulation by J. Carilli et al,, 1–5, doi:10.1002/(ISSN)1944-9186.

Karnauskas, K. B., A. L. Cohen, and J. M. Gove (2016), Mitigation of Coral Reef Warming Across the Central Pacific by the Equatorial Undercurrent: A Past and Future Divide, Nature, 6, 1–8, doi:10.1038/srep21213.

Karnauskas, K. B., and A. L. Cohen (2012), Equatorial refuge amid tropical warming, Nature Climate change, 2(7), 530–534, doi:10.1038/nclimate1499.

Karnauskas, K. B., R. Seager, A. Kaplan, Y. Kushnir, and M. A. Cane (2009), Observed Strengthening of the Zonal Sea Surface Temperature Gradient across the Equatorial Pacific Ocean, J. Climate, 22(16), 4316–4321, doi:10.1175/2009JCLI2936.1.

Karnauskas, K. B., S. Jenouvrier, C. W. Brown, and R. Murtugudde (2015b), Strong sea surface cooling in the eastern equatorial Pacific and implications for Galapagos Penguin conservation, Geophys. Res. Lett., 42(15), 6432–6437, doi:10.1002/2015GL064456.

Kessler, W. S. (2006), The circulation of the eastern tropical Pacific: A review, Progress in Oceanography, 69(2-4), 181–217, doi:10.1016/j.pocean.2006.03.009.

Linsley, B. K., P. Zhang, A. Kaplan, S. S. Howe, and G. M. Wellington (2008), Interdecadal-decadal climate variability from multicoral oxygen isotope records in the South Pacific Convergence Zone region since 1650 A.D, Paleoceanography, 23(2), 1–16, doi:10.1029/2007PA001539.

Lukas, R. (1986), The termination of the equatorial undercurrent in the eastern Pacific, Progress in Oceanography, doi:10.1016/0079-6611(86)90007-8.

L'Heureux, M. L., D. C. Collins, and Z.-Z. Hu (2012), Linear trends in sea surface temperature of the tropical Pacific Ocean and implications for the El Niño-Southern Oscillation, Clim Dyn, 40(5-6), 1223–1236, doi:10.1007/s00382-012-1331-2.

Mann, M. E., and P. D. Jones (2003), Global surface temperatures over the past two millennia, Geophys. Res. Lett., 30(15), 1–4, doi:10.1029/2003GL017814.

National Geophysical Data Center (2006), 2-minute Gridded Global Relief Data (ETOPO2) v2,, doi:10.7289/V5J1012Q.

Nurhati, I. S., K. M. Cobb, and E. Di Lorenzo (2011), Decadal-Scale SST and Salinity Variations in the Central Tropical Pacific: Signatures of Natural and Anthropogenic Climate Change, J. Climate, 24(13), 3294–3308, doi:10.1175/2011JCLI3852.1.

Reynolds, R. W., T. M. Smith, C. Liu, D. B. Chelton, K. S. Casey, and M. G. Schlax (2007), Daily High-Resolution-Blended Analyses for Sea Surface Temperature, J. Climate, 20(22), 5473–5496, doi:10.1175/2007JCLI1824.1.

Sayani, H. R., K. M. Cobb, A. L. Cohen, W. C. Elliott, I. S. Nurhati, R. B. Dunbar, K. A. Rose, and L. K. Zaunbrecher (2011), Effects of diagenesis on paleoclimate reconstructions from modern and young fossil corals, Geochimica et Cosmochimica Acta, 75(21), 6361–6373, doi:10.1016/j.gca.2011.08.026.

Schrag, D. P. (1999), Rapid analysis of high-precision Sr/Ca ratios in corals and other marine carbonates, Paleoceanography, 14(2), 97–102, doi:10.1029/1998PA900025.

Shen, G. T., J. E. Cole, D. W. Lea, L. J. Linn, T. A. McConnaughey, and R. G. Fairbanks (1992), Surface ocean variability at Galapagos from 1936–1982: Calibration of geochemical tracers in corals, Paleoceanography, 7(5), 563–588, doi:10.1029/92PA01825.

Strub, P. T., J. M. Mesias, V. Montecino, J. Rutillant, and S. Salinas (1998), Coastal ocean circulation off western South America, in The Sea, vol. 11, edited by A. R. Robinson and K. H. Brink, pp. 273–314, New York.

Sweet, W. V., J. M. Morrison, D. Kamykowski, B. A. Schaeffer, S. Banks, and A. McCulloch (2007), Water mass seasonal variability in the Galapagos archipelago, Deep-Sea Research Part I, 54(12), 2023–2035, doi:10.1016/j.dsr.2007.09.009.

Thirumalai, K., A. Singh, and R. Ramesh (2011), A MATLAB™ code to perform weighted linear regression with (correlated or uncorrelated) errors in bivariate data, J. Geol. Soc. India, 77(4), 377–380, doi:10.1007/s12594-011-0044-1.

Thompson, D. M., J. E. Cole, G. T. Shen, A. W. Tudhope, and G. A. Meehl (2015), Early twentieth-century warming linked to tropical Pacific wind strength, Nature Geoscience, 8(2), 117–121, doi:10.1038/ngeo2321.

Tierney, J. E., N. J. Abram, and K. J. Anchukaitis (2015), Tropical sea surface temperatures for the past four centuries reconstructed from coral archives, Paleoceanography, 30(3), 226–252, doi:10.1002/2014PA002717.

Toggweiler, J. R., and K. Dixon (1991), The Peru Upwelling and the Ventilation of the South Pacific Thermocline, J. Geophys. Res., 96, 20,467–20,497.

Vecchi, G. A., A. Clement, and B. J. Soden (2008), Examining the Tropical Pacific's Response to Global Warming, Eos, Transactions American Geophysical Union, 89(9), 81–83, doi:10.1029/2008EO090002.

Vecchi, G. A., and B. J. Soden (2007), Global warming and the weakening of the tropical circulation, J. Climate, 20(17), 4316–4340, doi:10.1175/JCLI4258.1.

Wallace, J. M., T. P. Mitchell, and C. Deser (1989), The Influence of Sea-Surface Temperature on Surface Wind in the Eastern Equatorial Pacific - Seasonal and Interannual Variability, J. Climate, 2(12), 1492–1499, doi:10.1175/1520-0442(1989)002<1492:TIOSST>2.0.CO;2.

Wolff, M. (2010), Galapagos does not show recent warming but increased seasonality, Galápagos Research, 67, 38–44.

Wu, H. C., M. Moreau, B. K. Linsley, D. P. Schrag, and T. Corrège (2014), Investigation of sea surface temperature changes from replicated coral Sr/Ca variations in the eastern equatorial Pacific (Clipperton Atoll) since 1874, Palaeogeography, Palaeoclimatology, Palaeoecology, 412(C), 208–222, doi:10.1016/j.palaeo.2014.07.039.

Xie, S.-P., C. Deser, G. A. Vecchi, J. Ma, H. Teng, and A. T. Wittenberg (2010), Global Warming Pattern Formation: Sea Surface Temperature and Rainfall, J. Climate, 23(4), 966–986, doi:10.1175/2009JCLI3329.1.

Yeh, S. W., J. S. Kug, B. Dewitte, M. H. Kwon, and B. P. Kirtman (2009), El Niño in a changing climate, Nature, 461(7263), 511–514, doi:10.1038/nature08316.

Zhang, G. J., and M. J. McPhaden (1995), The relationship between sea surface temperature and latent heat flux in the equatorial Pacific, J. Climate, 8(3), 589–605, doi:10.1175/1520-0442(1995)008<0589:TRBSST>2.0.CO;2.

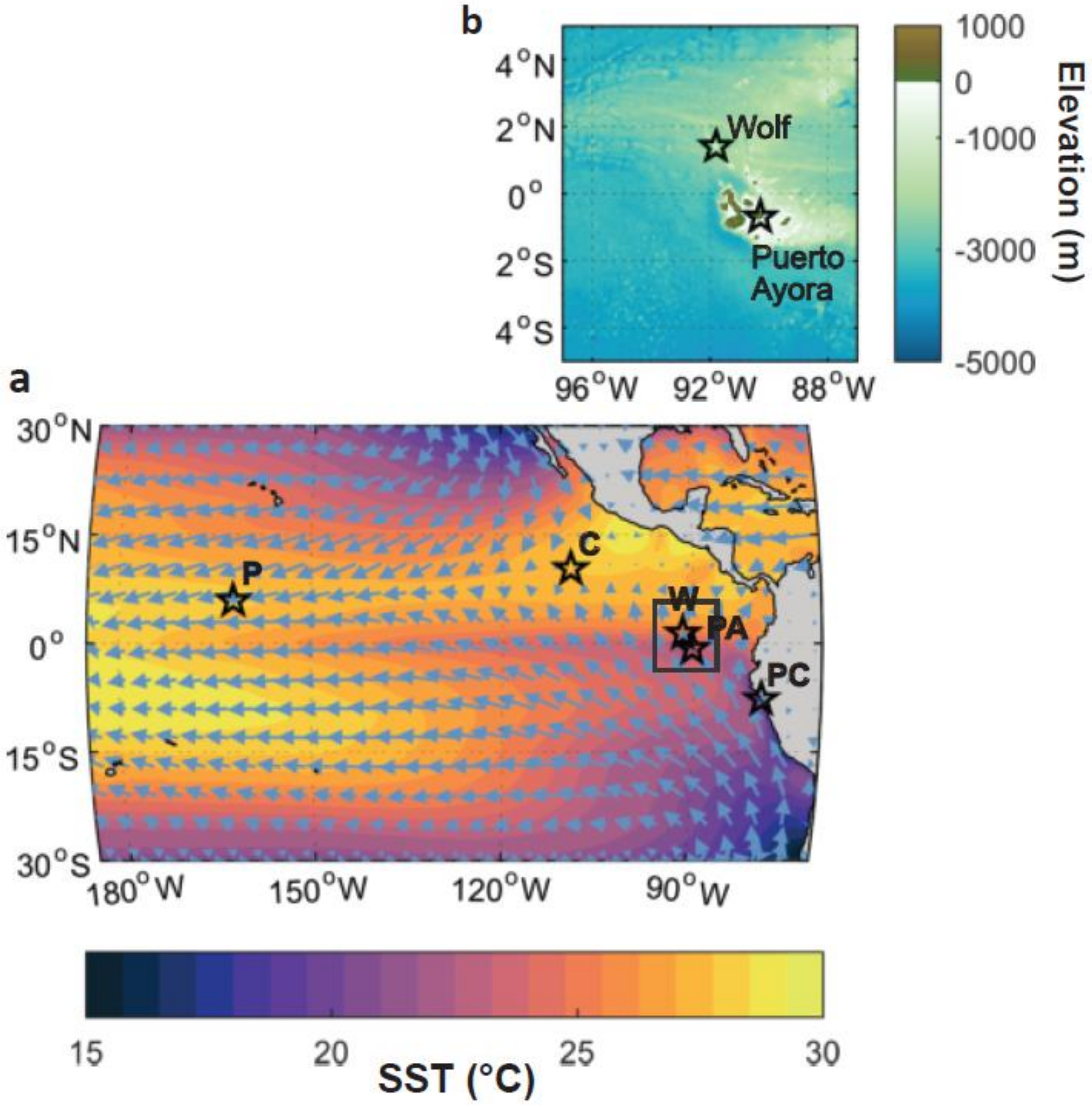

Figure 1. (a) Climatologic setting of the ETP. SSTs (colors) are the average of 0.25° Optimum Interpolation Sea Surface Temperature (OISST) from 1982-2014; winds (vectors) are the 1000 mbar average over the same period from the 2° National Oceanic and Atmospheric Administration 20th Century Reanalysis (20CR) v2 (Compo et al., 2011). Longest vector is 9.5 m/s; for display, vectors in all figures are cubically interpolated to 50% spatial resolution. **(b)** Expanded map from box in (a) shows Galápagos bathymetry from the National Geophysical Data Center 2-minute Gridded Global Relief Data v2 (2006). In all figures, stars indicate coral and instrumental sites (C: Clipperton, P: Palmyra, PA: Puerto Ayora, PC: Puerto Chicama, and W: Wolf).

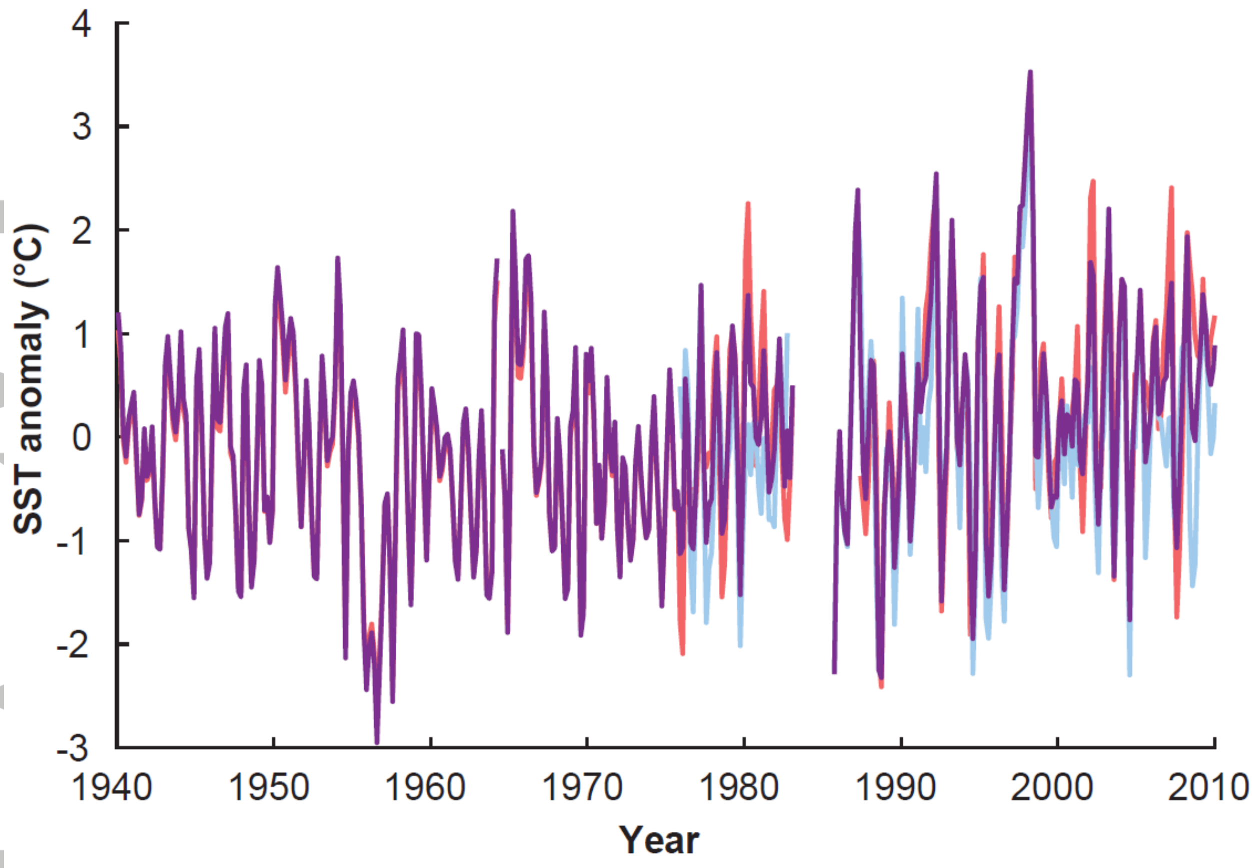

Figure 2. Bimonthly reconstructed SST anomalies (relative to mean bimonthly values) for the Wolf composite record (Sr/Ca = 10.66-0.057*SST), showing the composite (purple), GW10-3 (blue), and GW10-10 (light red). The 1982-83 El Niño caused a growth hiatus from 1983-1985.

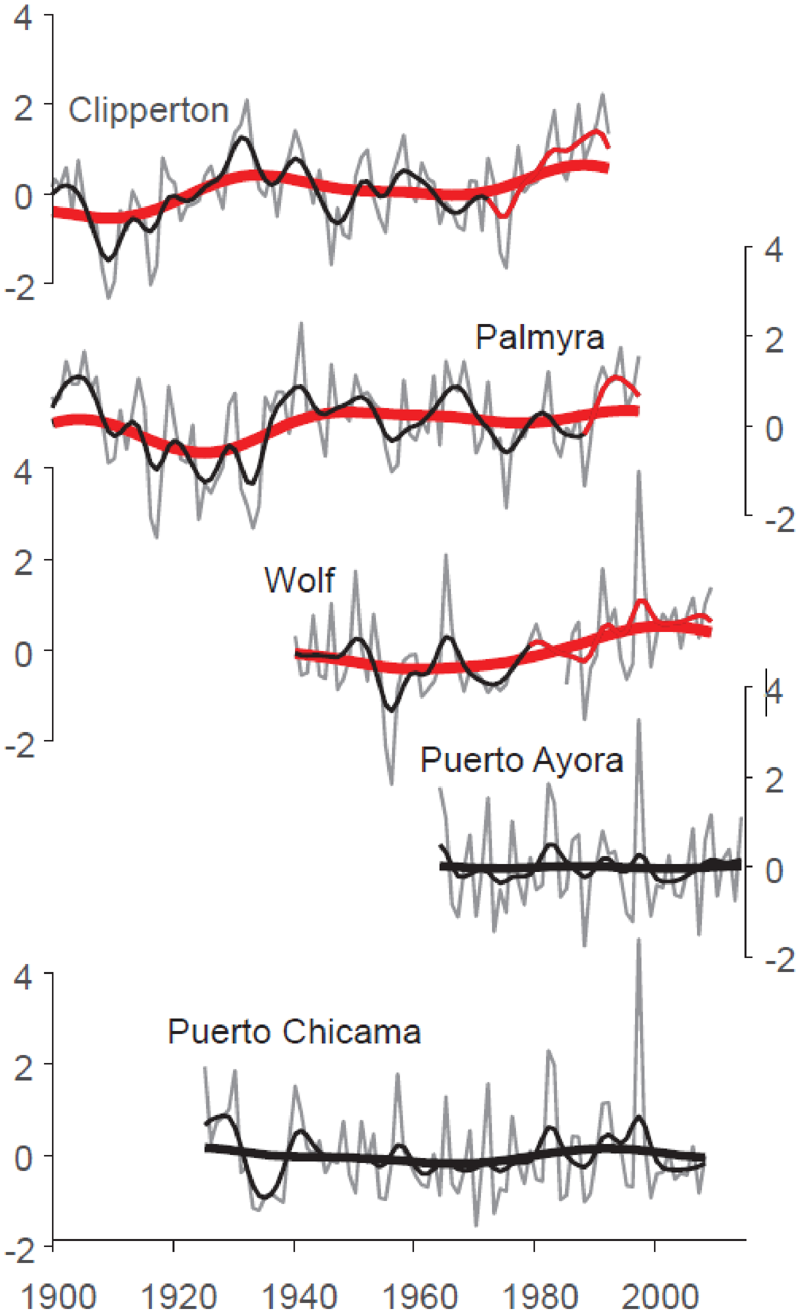

Figure 3. Trends in ETP proxy and instrumental records: tropical year averaged series (grey lines), 10-year Gaussian smoothed series (thin black/red lines), and 50-year Gaussian smoothed series (thick black/red lines). Lines are red where SiZer identified significant trends (p<0.1).

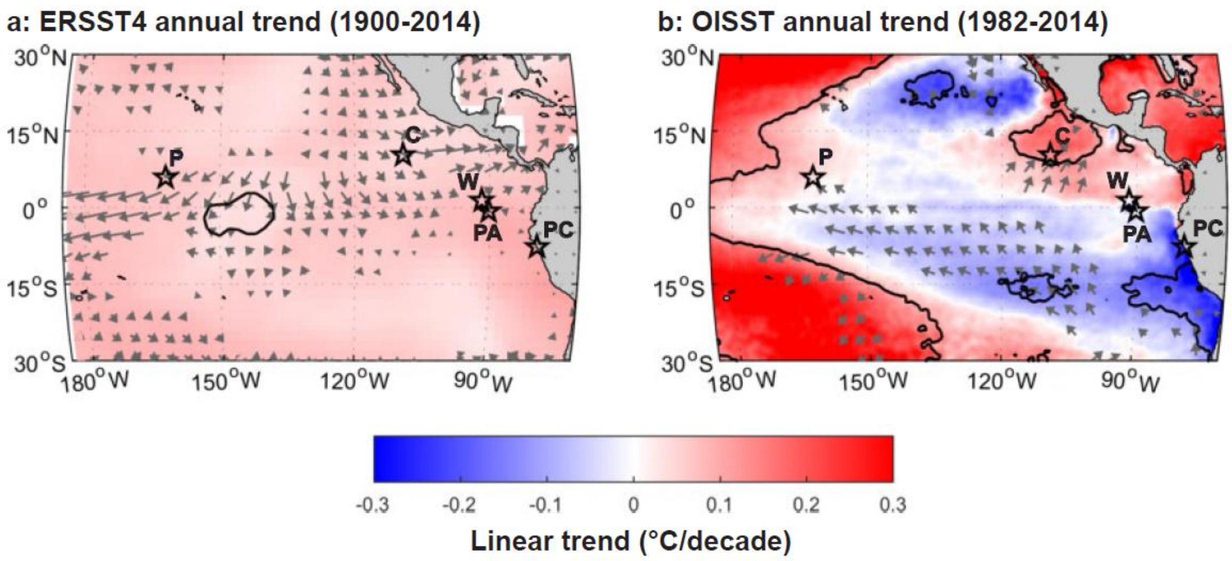

Figure 4. Linear trends in in tropical year-averaged ETP SST gridded datasets (colors). Contours indicate significance at $p<0.05$ (in (a), significant area is outside contoured shape). Vectors show significant linear trends ($p<0.05$) in 20CR v2 winds at 1000 mbar; longest vector (in (a)) is 3.8 m/s.

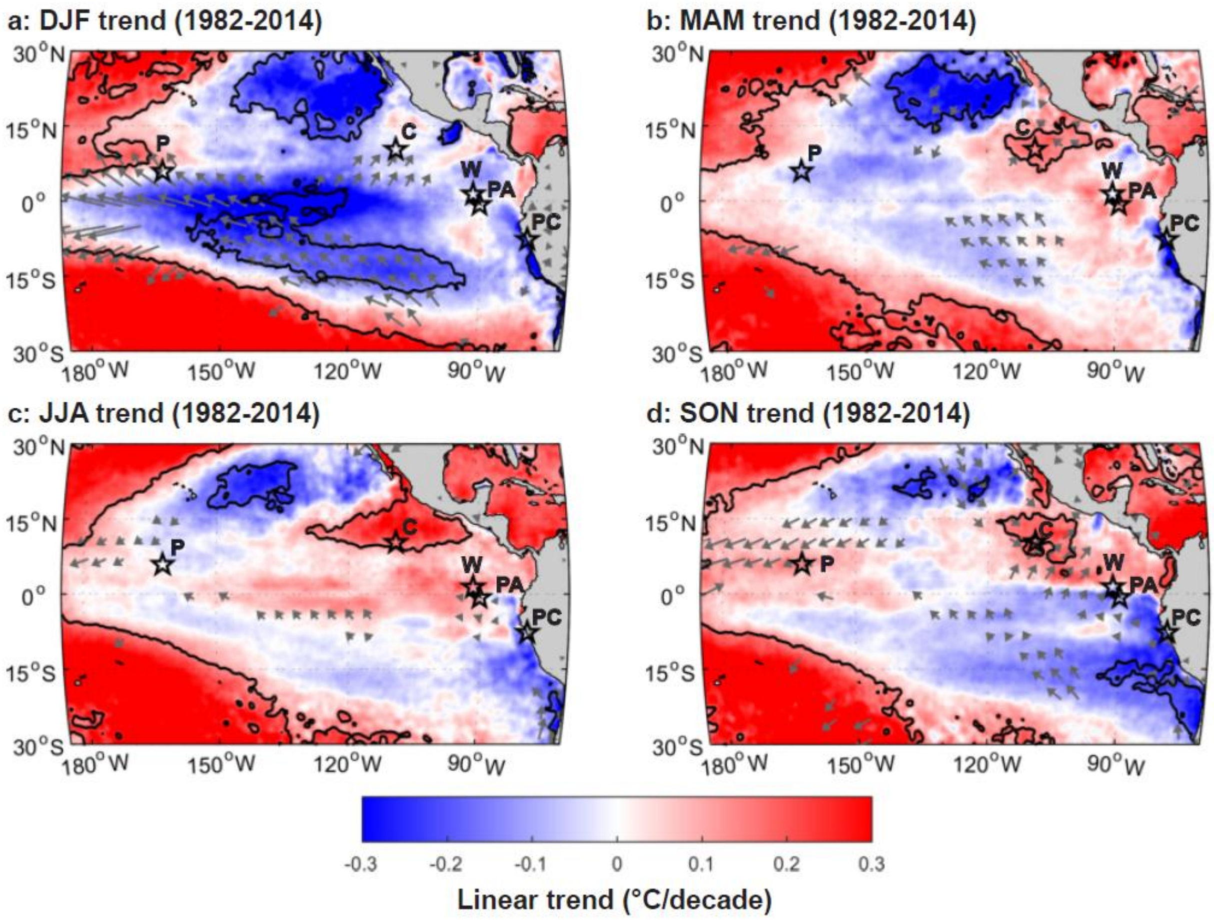

Figure 5. Linear trends in seasonal OISST from 1982-2014 (colors; contours indicate significance at $p<0.05$), for **(a)** DJF, **(b)** MAM, **(c)** JJA, and **(d)** SON. During the same seasons, vectors show significant linear trends ($p<0.05$) in 20CR v2 winds at 1000 mbar; longest vector (in (a)) is 5.5 m/s.